available at www.sciencedirect.com

ScienceDirect

journal homepage: www.elsevier.com/locate/ecolmodel

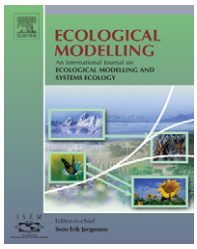

Simulation of NO and N_2O emissions from a spruce forest during a freeze/thaw event using an N-flux submodel from the PnET-N-DNDC model integrated to CoupModel

Josefine Norman[a,*], *Per-Erik Jansson*[b], *Neda Farahbakhshazad*[b], *Klaus Butterbach-Bahl*[c], *Changsheng Li*[d], *Leif Klemedtsson*[a]

[a] *Department of Plant and Environmental Sciences, University of Gothenburg, P.O. Box 461, SE-405 30 Gothenburg, Sweden*

[b] *Department of Land and Water Resources Engineering, Royal Institute of Technology (KTH), SE-100 44 Stockholm, Sweden*

[c] *Division Biosphere/Atmosphere Exchange, Department of Soil Microbiology, Fraunhofer Institute for Atmospheric Environmental Research (IFU), Garmisch-Partenkirchen, Germany*

[d] *Institute for the Study of Earth, Oceans, and Space, Complex Systems Research Center, University of New Hampshire, Durham, NH 03824, USA*

ARTICLE INFO

Article history:
Received 4 January 2007
Received in revised form
11 April 2008
Accepted 22 April 2008
Published on line 6 June 2008

Keywords:
Forest ecosystem modelling
NO emission
N_2O emission
CoupModel
DNDC model

ABSTRACT

The amount of nitrogen gases (N_2O, NO and N_2) emitted from forest soils depends on interactions between soil properties, climatic factors and soil management. To increase the understanding of nitrogen processes in soil ecosystems, two dynamic models, CoupModel (coupled heat and mass transfer model for soil–plant–atmosphere systems) and the denitrification–decomposition (DNDC) model were selected. Both are dynamic models with different submodels for soil, vegetation, hydrology and climate system. CoupModel has a higher degree of detail on soil physical and abiotic components, whereas the DNDC model contains details of microbiological processes involved in production of nitrogen gases. To improve the previous simple submodel of nitrogen emission in CoupModel, we included a submodel corresponding to the forest version of DNDC containing photosynthesis/evapotranspiration-nitrogen (PnET-N-DNDC model).

The nitrogen (N) and carbon (C) submodel of CoupModel was parameterised with respect to the parameter values in PnET-N-DNDC. In addition, a simple kinetic scheme for estimating of the size of the anaerobic fraction in soil (anaerobic balloon) was adopted from PnET-N-DNDC.

Climate and soil data from a spruce (*Picea abies*) forest were used for analysing differences between the modified CoupModel and PnET-N-DNDC regarding emissions of NO and N_2O from nitrification and denitrification. The used simulation period contains an extreme event with a 4-month with frozen soil and an overlap of continually a 4-month high N_2O emission. The validation outputs were soil temperature (5 depths), water content (2 depths), and the emission rates of NO and N_2O. To describe gas exchange from anaerobic to aerobic sites, we added a new parameter in CoupModel that enabled the model to emit N-gases even when the soil was completely saturated. The modification allows spatial soil heterogeneity in a conceptual way and improved estimation of N_2O gas. The NO gas content was

* *Corresponding author*. Tel.: +46 31 773 29 28; fax: +46 31 773 29 84.
E-mail address: josefine.norman@botany.gu.se (J. Norman).

doi:10.1016/j.ecolmodel.2008.04.012

almost unchanged in simulations due to the majority being formed during nitrification. The simulated accumulated amount of N_2O varied between an underestimation of −41% and an overestimation of 15% to from the field data. For the accumulated NO emission differences between the simulations were smaller, from −15% to 18%. This provided the possibility to further investigate CoupModel's potential in describing N emissions during denitrification from different ecosystems.

The system proved to be sensitive to additional N deposition, and increasing available N, for nitrification and denitrification in thawing conditions forced CoupModel to emit NO and N_2O earlier in the spring.

1. Introduction

The nitrogen trace gases nitric oxide (NO) and nitrous oxide (N_2O) are both products of two main microbial metabolic pathways in the soil; nitrification and denitrification (Firestone and Davidson, 1989). According to IPCC (2001b), NO has a mean residence time of less than 3 days in the atmosphere, reacts rapidly and is involved in the production of trophospheric ozone. On the other hand, N_2O has a residence time of 120 years and contributes to the greenhouse effect (IPCC, 2001b) due to its enormous global warming potential of 290 times that of CO_2. Thus, there has been an increasing interest in understanding the nitrogen cycle and how it has been affected by anthropogenic activities in terrestrial ecosystems (IPCC, 2001a). The nitrogen cycle in general and the processes generating trace gases in particular are complicated as they are driven by a large number of variables, which are further linked in a complex manner. Robertson (1989) introduced schematic diagrams of nitrification and denitrification showing that climate factors (i.e. rainfall and temperature), disturbance factors for the plant community structure and soil type (i.e. soil organic matter, mineralogy, and pH) all are of great importance for the biological and chemico-physical processes involved in biosphere–atmosphere exchange of trace gases. The system is even more complicated considering that nitrification is an aerobic process that requires oxygen, whereas denitrification is an anaerobic process, forming gases when oxygen is absent.

Traditional statistical or simple empirical models are good tools for predicting greenhouse gas exchange for specific sites and ecosystems (Conen et al., 2000a,b). However, there is a demand for models that mirror our understanding of the processes involved, thereby improving utilisation of the large amounts of measured data from various ecosystems. These can further be used to predict effects of future climate change on emissions of greenhouse gases from terrestrial ecosystems. To achieve this, the models have to be mechanistically capable of replicating processes in the soil and utilising large amounts of data, in order to handle the temporal and spatial aspects of the flux estimates. Most mechanistic ecosystem models are restricted as regards their suitability for prediction of greenhouse gas emissions, and a great number of models diverge in their formulation of nutrient cycling, but are attuned in water and carbon processes (Tiktak and van Grinsven, 1995). For example, Potter et al. (2000) and Parton et al. (2001) each developed a full ecosystem model, but the approach describing the emission of gaseous nitrogen fluxes from the soils differed. However, other mechanistic models have been created where the focus is on understanding/describing microbial processes rather than describing the other components of the soil biogeochemical cycle. Henault and Germon (2000) first created a model predicting N_2O emissions from denitrification for agricultural systems, which was later expanded to include an algorithm calculating N_2O emissions from nitrification (Henault et al., 2005). These models calculated denitrification and nitrification rates from biological parameters (e.g. maximum potential denitrification rate), water-filled pore space (WFPS), temperature and mineral nitrogen content. The approach in these models, as well as in a comparable model developed by Langeveld and Leffelaar (2002), was to simulate N_2O emissions from denitrification for homogeneous soils, and the specific focus was on the random distribution of water and air-filled pores therein.

CoupModel, used in the current investigation, originated from the SOIL model on water and heat first presented by Jansson and Halldin (1979) and its sister model SOILN, first presented by Johnsson et al. (1987). Later a crop growth model (Eckersten et al., 1998) was added to CoupModel. The full CoupModel has been presented by Jansson and Moon (2001) and a detailed description by Jansson and Karlberg (2004) is also available on the internet.

Prior to the present study, CoupModel lacked the capacity to explicitly quantify emissions of NO, N_2O, and N_2 gases from soils. This was rectified by adopting a detailed submodel of nitrification, denitrification and gas fluxes from the PnET-N-DNDC model (Li et al., 2000). PnET-N-DNDC is the forest version of the DNDC model (Li et al., 1992, 2000). Compared with CoupModel, PnET-N-DNDC is less focused on describing abiotic components and processes, but contains a detailed submodel for describing nitrification and denitrification processes. These processes are governed by microbial dynamics and environmental factors such as pH, water content and temperature in the soil. It also adds an oxygen diffusion algorithm, which is a key factor regulating the denitrification sequence and defines the size of volumetric fraction of anaerobic microsites by tracking the size of an anaerobic balloon (Li et al., 2000). This allows the simultaneous occurrence of aerobic (e.g. nitrification) and anaerobic (e.g. denitrification) microbial processes in the same soil layer. The nitrification and denitrification submodel was implemented in CoupModel, since it is a mechanistic model developed for various ecosystems and since it has been previously tested for up-scaling of nitrogen trace gas emissions, e.g. from forests (Stange et al., 2000), wetlands (Zhang et al., 2002b) and agricultural systems (Butterbach-Bahl et al., 2004).

The aim of the present study was to develop an improved understanding of nitrogen emissions from forest soils by introducing an existing component from the PnET-N-DNDC model into CoupModel. For this approach we used climate forcing data, combined with a description of physical and biological processes from an old spruce forest in southern Germany. We simulated the period April 1995 to April 1997, but focused on a coherent period of clear connections between NO and N_2O emissions during summer and winter, as observed for the period July 1995 to July 1996. In this paper, we compare three different parameterisations of CoupModel (option A, B, and C) with the original application of PnET-N-DNDC for the Höglwald site. Option A of CoupModel directly adopted the anaerobic balloon concept of PnET-N-DNDC, whereas option B differed in parameter setup and modified the exchange rate between the anaerobic and aerobic sites of the soil. Option C was similar to option B, but represented an optional enhanced dry nitrogen deposition rate, to demonstrate the sensitivity of the nitrogen balance of the system to the available inorganic nitrogen in the soil. We compared the advantages and disadvantages of using different models for estimation of nitrogen emissions, depending on the specific purpose and availability of data.

2. Materials and methods

2.1. Site description

To compare the PnET-N-DNDC model and CoupModel, we used data from a spruce site in the Höglwald forest, Germany (48°30′N, 11°10′E). It is an almost 100-year-old spruce stand, with a standing height of approximately 35 m at the time of measuring. The mineral soil is a loam with clay/sand fractions of 0.05/0.64 at 0–10 cm, 0.11/0.5 at 10–20 cm and 0.22/0.48 at 20–40 cm, with an overlying organic layer of approximately 4 cm depth (containing 30 t C ha^{-1}). Measurements of NO and N_2O fluxes were made using 5 fully automatic chambers with

Table 1 – List of equations

Equation		Definition
Nitrification		
$N_{NH_4\rightarrow NO_3} = n_m f(T) f(\theta) f(N_{NH_4}) n_{pH} N_m$	(1)	Nitrification rate
$f(N_{NH_4}) = \frac{N_{NH_4}/(\theta\,\Delta z)}{(N_{NH_4}/(\theta\,\Delta z)) + n_h}$	(2)	Response function for ammonium concentration
$\frac{\Delta N_{micrN}}{\Delta t} = M_g - M_d - M_r$	(3)	Biomass of nitrification microbes
$M_g = n_n f(T) f(\theta) f(C) f(N_{NO_3}) n_{pH} N_m$	(4)	Growth rate of nitrification microbes
$M_d = n_d f(T) f(\theta) f(C) n_{pH} N_m^2$	(5)	Death rate of nitrification microbes
$M_r = n_d f(T) f(\theta) n_{pH} \left(\frac{1}{cn_m} - 1\right) N_m$	(6)	Respiration rate of nitrification microbes
Denitrification		
$N_{NO_3\rightarrow AnNO_2} = (N_{rgNO_3} + N_{rmNO_3}) M_a N_d$	(7)	Flux from NO_3 to NO_2 in the anaerobic balloon
$N_{AnNO_2\rightarrow AnNO} = (N_{rgNO_2} + N_{rmNO_2}) M_a N_d$	(8)	Flux from NO_2 to NO in the anaerobic balloon
$N_{AnNO\rightarrow AnN_2O} = (N_{rgNO} + N_{rmNO}) M_a N_d$	(9)	Flux from NO to N_2O in the anaerobic balloon
$N_{AnN_2O\rightarrow AnN_2} = (N_{rgN_2O} + N_{rmN_2O}) f(N_{NO_3Conc}) M_a N_d$	(10)	Flux from N_2O to N_2 in the anaerobic balloon
$N_{rg} = d_g f(C) f(N_c) \frac{M_a N_d}{d_e}$	(11)	Growth respiration for denirtification microbes
$N_{rm} = \frac{d_r N}{N_{An}}$	(12)	Maintenance respiration for denitrification microbes
$M_a = f(T) f(pH) f(N_{An}) f_A(z) d_{ac}$	(13)	Denitrification microbial activity
Gas flux		
$N_{NO_3\rightarrow NO} = g_f f(T) f(pH) \left(1 - \frac{1}{1 + e^{(\theta(z) - g_{\theta c})/g_{\theta f}}}\right) N_{NH_4\rightarrow NO_3}$	(14)	NO emission rate from nitrification
$N_{NO_3\rightarrow N_2O} = g_f f(T) \left(1 - \frac{1}{1 + e^{(\theta(z) - g_{\theta c})/g_{\theta f}}}\right) N_{NH_4\rightarrow NO_3}$	(15)	N_2O emission rate from nitrification
$f_A = \exp(-g O_v^2)$	(16)	Volumetric anaerobic fraction
$N_{AnGas\rightarrow Gas} = \min(f(O_2) N_{An},\ 0.5 N_{An})$	(17)	NO, N_2O and N_2 formed during denitrification
$f(O_2) = f_A(1 - f_A) O_r o_d$	(18)	Oxygen diffusion exchange function
$O_r = d_{O_2} f_a o_{dc} D$	(19)	Oxygen diffusion rate
$f(O_2) = o_b + f_A(1 - f_A) O_r o_d$	(20)	New function of oxygen diffusion exchange

Definitions of symbols; state and flow variables are denoted by upper case subscripted with name abbreviation, auxiliary variables also representing functions are denoted by lower case followed by brackets containing a list a of dependent variables, parameters are denoted by lower case letters. Lower case f is used both to denote fraction or as a general symbol for function. A full explanation for each symbol is given in the text when not obvious from definition of equation.

possibilities to measure approximately 60 flux rates per day for N_2O and twice as much for NO (Butterbach-Bahl et al., 1997, 1998). A triplicate of time domain reflectometry (TDR) probes were used to measure volumetric water of two depths (Rothe, 1997). These values were transformed to WFPS using bulk density values (Breuer et al., 2000). The annual wet nitrogen deposition in through fall at the site is 30–35 kg N/ha and soil pH (in $CaCl_2$) is 3.2. Meteorological data for the period April 1995 to April 1997 were used in the simulations with annual mean temperature of 7.3 °C and annual precipitation of 800 mm. The site is described in greater detail by Kreutzer (1995), Butterbach-Bahl et al. (1997), Papen and Butterbach-Bahl (1999) and Li et al. (2000).

2.2. *Model description*

The PnET-N-DNDC model is made up of three parts: (1) *PnET*, the photosynthesis–evapotranspiration model, describing photosynthesis, respiration, organic carbon production and allocation and litter production for forest ecosystems (Aber and Federer, 1992); (2) *N*, the nitrification model, predicting nitrifier growth/death rate, nitrification rate and emissions of NO and N_2O from this process (Stange, 2001); and (3) *DNDC*, the denitrification–decomposition model, a biogeochemical model with links between ecological drivers, environmental factors and decomposition, as well as denitrification with emissions of NO and N_2O (Li et al., 1992).

Table 2 – List of parameters

Symbol	Explanation	Value	Unit	Equation	Comments
Nitrification					
n_m	Nitrification rate coefficient	0.25	mg ha day^{-1} kg^{-1}	(1)	Default
n_{pH}	Coefficient for pH response on nitrification	1	–	(1), (5), (6)	Default
n_h	Half rate of ammonium	6.18	mg N l^{-1}	(2)	
n_n	Growth coefficient for nitrifiers	2	day^{-1}	(4)	Default
n_d	Death coefficient for nitrifiers	1	day^{-1}	(5), (6)	Default
cn_m	Fixed carbon nitrogen ratio of microbes	10	–	(6)	Default
Denitrification					
$d_g(NO_3)$	Growth parameter for NO_3 during denitrification	4	day^{-1}	(11)	Default
$d_g(NO_2)$	Growth parameter for NO_2 during denitrification	4	day^{-1}	(11)	Default
$d_g(NO)$	Growth parameter for NO during denitrification	32.8	day^{-1}	(11)	Default
$d_g(N_2O)$	Growth parameter for N_2O during denitrification	32.8	day^{-1}	(11)	Default
$d_e(NO_3)$	Efficiency parameter for NO_3 during denitrification	4.28	day^{-1}	(11)	Default
$d_e(NO_2)$	Efficiency parameter for NO_2 during denitrification	4.28	day^{-1}	(11)	Default
$d_e(NO)$	Efficiency parameter for NO during denitrification	0.151	day^{-1}	(11)	Default
$d_e(N_2O)$	Efficiency parameter for N_2O during denitrification	0.151	day^{-1}	(11)	Default, Van Verseveld et al. (1977)
$d_r(NO_3)$	Respiration parameter for NO_3 during denitrification	0.55	day^{-1}	(12)	Default
$d_r(NO_2)$	Respiration parameter for NO_2 during denitrification	0.21	day^{-1}	(12)	Default
$d_r(NO)$	Respiration parameter for NO during denitrification	3.36	day^{-1}	(12)	Default
$d_r(N_2O)$	Respiration parameter for N_2O during denitrification	7.6	day^{-1}	(12)	Default
d_{ac}	Denitrification activity rate coefficient	0.5	day^{-1}	(13)	Default
Gas flux					
g_f	Maximum NO fraction	0.004	–	(14)	Baumgärtner and Conrad (1992)
$g_{\theta c}$	Relative saturation level for NO when the response is 50% for soil moisture in the formation of nitrous trace gases	0.45	–	(14)	DNDC, Stange (2001)
$g_{\theta f}$	Shape parameter for the moisture response function of function of the formation of NO in the nitrification	0.024	–	(14)	DNDC, Stange (2001)
g_f	Maximum N_2O fraction	0.0006	–	(15)	DNDC
$g_{\theta c}$	Relative saturation level for N_2O when the response is 50% for soil moisture in the formation of nitrous trace gases	0.55	–	(15)	DNDC Stange (2001), Maag and Vinther (1996)
$g_{\theta f}$	Shape parameter for the moisture response function of formation of N_2O in the nitrification	0.24	–	(15)	DNDC Stange (2001), Maag and Vinther (1996)
g	Shape parameter for the function describing anaerobic fraction at different oxygen levels in the anaerobic balloon	200	–	(16)	Default
o_d	Oxygen diffusion reduction parameter	$0.01/5e^{-4}$	–	(18), (20)	DNDC/CoupModel design
d_{O_2}	Tortuosity of O_2 depending on the soil formation	0.1	–	(19)	Default
o_b	Base level of oxygen diffusion function	$-/5e^{-5}$	–	(20)	DNDC/CoupModel design

CoupModel represents a flexible coupling between heat and mass transfer for soil–plant–atmosphere systems, where interactions between different components are considered. The model allows for simulation of different spatial and temporal scales, and is well adapted to consider winter conditions with snow and frost. The input data are described either as parameters or by measured variables (Jansson and Karlberg, 2004).

Presented equations in Table 1 can easy be linked to list of parameters (Table 2) and list of variables (Table 3).

2.3. *Water and heat processes*

Water and heat processes are fundamental components of any model that aims to describe nitrogen gas emissions. Both models used in this study have a one-dimensional water and heat transfer algorithm, designed to calculate flows in the profile with respect to gradients. CoupModel is close to a classical numerical solution of Richards's equation, which also allows the soil profile to be completely saturated, whereas PnET-N-DNDC represents a simplified scheme for unsaturated soils. The profile in CoupModel is divided into a user-defined number of soil layers with flexible compartment sizes, depending on available information from the specific site. In this case we used 15 layers to 7 m depth with an upper 3 cm layer and following layers increasing in thickness with depth. The DNDC model is more specifically developed for regional applications, and has a limited range of defined soil environments. The modelled soil in DNDC is divided into a series of horizontal layers, in this case 17 layers of 2.14 cm each, with uniform temperature and moisture content. Water and heat fluxes between layers are determined by gradients of soil water potential and soil temperature. Water flow from the bottom of the soil profile is driven by gravity drainage (Li et al., 1992).

The water transfer part of CoupModel handles surface and soil layer pools with incoming and outgoing water to the system. Water addition is by irrigation/precipitation (water or snow) and groundwater inflow, whereas removal of water is by evapotranspiration, surface runoff, water uptake by roots, groundwater outflow and percolation. The shallow profile depth in the DNDC model only has vertical water flows, whereas CoupModel has a combination of vertical and horizontal water flows with a dynamic groundwater level. CoupModel has an iterative energy balance at the soil surface to describe surface heat flux, whereas the DNDC model assigns the soil surface the mean daily temperature. The lower boundary for heat is a pre-defined temperature, in DNDC at a depth of 5 m.

Plant cover and surface water have specific area representation in CoupModel, whereas only a homogeneous plant cover is considered in PnET-N-DNDC. Losses of rain and snow by transpiration and interception are described as dynamic processes in CoupModel, while they have been given more static descriptions in PnET-N-DNDC (Aber and Federer, 1992). In CoupModel the forest is described with a forest floor and a tree canopy, with separate extension in both height and surface cover (Jansson and Karlberg, 2004).

The soil texture and organic matter content are strongly relevant for the soil moisture content. In CoupModel, each soil layer has to be assigned specific water retention curves, which can be calculated from functions or taken from a soil database. In DNDC there are 12 predefined soil textures eligible for the profile (Li et al., 1992).

2.4. *Nitrogen flux*

In both CoupModel and DNDC the nitrogen processes are divided into two parts, fluxes above and below ground. Processes above ground include external inputs, plant growth, soil managements and response functions for vegetation temperature and soil moisture. In these processes the amount of nitrogen and the C:N ratio together govern the amount of

Table 3 – List of variables

Variable	Unit	Equation
Response function of soil temperature, $f(T)$	–	(1), (4)–(6), (13)–(15)
Response function of soil moisture content, $f(\theta)$	–	(1), (4)–(6), (13)–(15)
Biomass of the microbial nitrifiers, N_m	$g\,m^{-2}$	(1), (4)–(6)
Ammonium content, N_{NH_4}	$g\,m^{-2}$	(2)
Soil moisture content, θ	vol.%	(2)
Soil layer, z	m	(2)
Response function of dissolved organic carbon concentration, $f(C)$	–	(4), (5), (11)
Response function of nitrate content, $f(N_{NO_3})$	–	(4)
Biomass of the microbial denitrifiers, N_d	$g\,m^{-2}$	(7)–(11)
Response function of nitrate concentration, $f(N_{NO_3Conc})$	–	(10)
Response function of nitrogen concentration, $f(N_c)$	–	(11)
Amount of nitrogen in NO_3, NO_2, NO and N_2O, N	$g\,m^{-2}$	(12)
Nitrogen content in the anaerobic nitrogen pools (NO_3, NO_2, NO and N_2O), N_{An}	$g\,m^{-2}$	(12), (17)
Response function of nitrogen content in the anaerobic nitrogen pools (NO_3, NO_2, NO and N_2O), $f(N_{An})$	–	(13)
Response function of soil pH, $f(pH)$	–	(13), (14)
Nitrification rate, $N_{NH_4\rightarrow NO_3}$	$g\,m^{-2}\,day^{-1}$	(14), (15)
Volumetric oxygen concentration, O_v	%	(16)
Volumetric anaerobic fraction, f_A	–	(18), (20)
Fraction of air-filled pores, f_a	–	(19)
Diffusion coefficient in free air, D	–	(19)

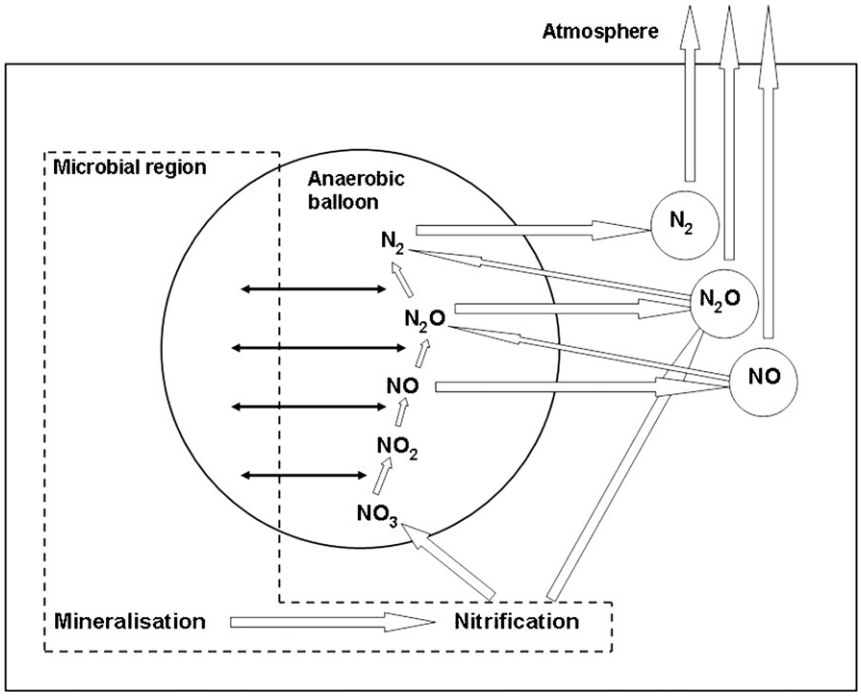

Fig. 1 – Schematic overview of the nitrogen emissions from the nitrification and denitrification processes in one soil layer in CoupModel. The anaerobic balloon represents a virtual volume of the soil that is considered anaerobic.

carbon in the system. Processes below ground include soil organic nitrogen and carbon dynamics, mineral nitrogen and gas processes. The inorganic processes, i.e. nitrification, denitrification and gas exchanges are shown in Fig. 1.

2.5. *Nitrification*

The chain of inorganic processes begins with the nitrification process where ammonium (NH_4^+) is converted to nitrate (NO_3^-) (Fig. 1). In this process, the rate of microbial activity is important and leads to secondary emissions of NO and N_2O. In the nitrification rate calculation (Eq. (1), Table 1), the microbes are explicitly involved and respond to temperature, moisture, pH and ammonium concentration in the soil. The ammonium concentration (Eq. (2), Table 1) is linked to the amounts of moisture in each layer in the soil profile.

Nitrifier biomass is dependent on their growth, death and respiration rates (Eq. (3), Table 1). The growth rate (Eq. (4), Table 1) is dependent on temperature, moisture, concentration of dissolved organic carbon and soil nitrate concentration responses. The death and respiration rates (Eqs. (5) and (6), Table 1) are not dependent on the soil nitrate concentration, but dependent on the temperature and moisture. The death rate is also related to the dissolved organic carbon concentration. All three rates (growth, respiration and death) are related to the previous biomass of the microbial nitrifiers (N_m) (Table 1).

The emission rates of NO and N_2O gases formed during nitrification are calculated in Eqs. (14) and (15), respectively (Table 1). Both emission rates are highly dependent on their own value of the maximum fraction parameter (g_f), i.e. the fraction of NO and N_2O loss from gross nitrification (Ingwersen et al., 1999). The temperature, moisture and pH responses of the soil are included in the NO emission rate calculation, whereas pH is excluded as an effect of the N_2O emission rate.

2.6. *Denitrification and gas fluxes*

Denitrification is the process whereby nitrate is converted to NO_2^-, NO, N_2O and N_2, at the anaerobic sites in the soil (Fig. 1). Soil microbes use nitrogen from the nitrogen gas pools (NO_2^-, NO, N_2O and N_2) and the NO_3^- pool for maintenance, growth and respiration. Loss of nitrogen in one pool act as a supply for the next pool in the denitrification chain ($NO_3^- \rightarrow NO_2^- \rightarrow NO \rightarrow N_2O \rightarrow N_2$). Fluxes of nitrogen from one pool to the next are calculated in Eqs. (7)–(10) (Table 1). The fluxes depend on biomass of the denitrifiers (N_d), microbial denitrification activities (Eq. (13)), growth respiration (Eq. (11)) and maintenance respiration (Eq. (12)) of the microbes. They are separately calculated for NO_3^-, NO_2^-, NO and N_2O, and have different parameters in efficiency, respiration and growth.

Microbial denitrification activity (Eq. (13), Table 1) is influenced by soil temperature, soil pH, content of nitrogen in the anaerobic pool and volumetric anaerobic fraction of the soil. The volumetric anaerobic fraction, i.e. the anaerobic balloon, is dependent on the volumetric oxygen concentration O_v, as well as the shape parameter, g (Eq. (16), Table 1).

Conceptually, each layer emits the nitrogen gases formed to the soil layer above, while the topsoil emits the gases directly to the atmosphere. The gases formed during denitrification, i.e. NO, N_2O and N_2, leave the anaerobic site to enter the aerobic gas pools and add to the gases formed during the

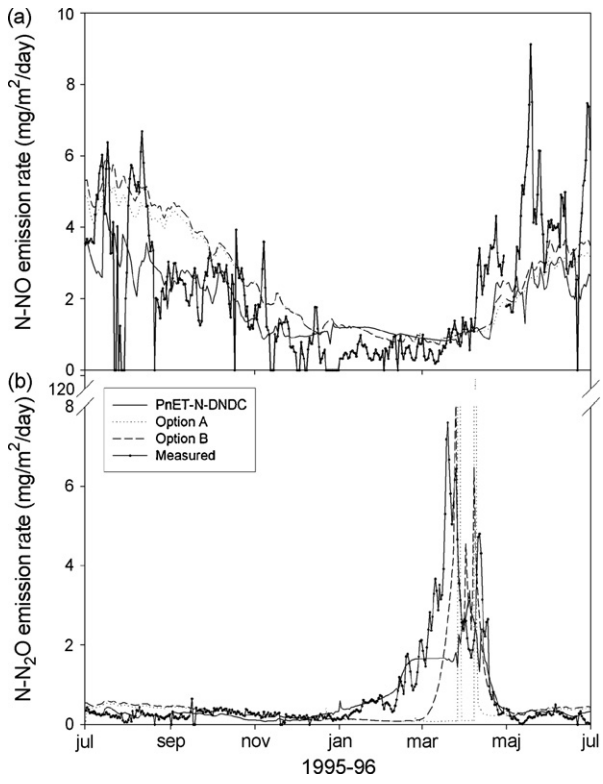

Fig. 2 – (a) NO emission rate and (b) N_2O emission rate for PnET-N-DNDC, options A and B, and measured data.

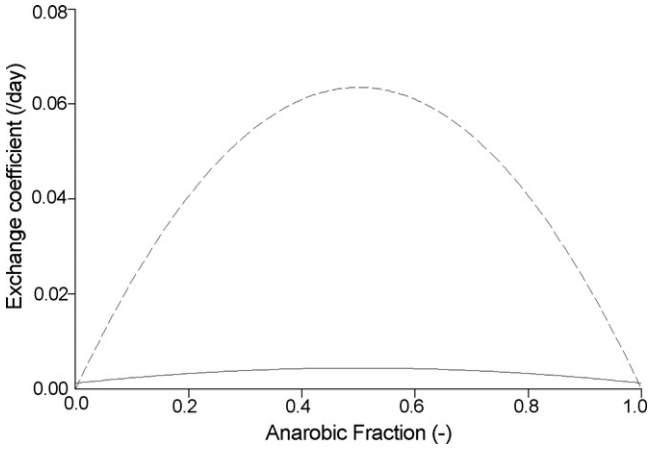

Fig. 3 – Oxygen diffusion exchange coefficient as a function of anaerobic volumetric fraction for option A (dashed line) and B (solid line).

nitrification. This transport is calculated analogously for NO, N_2O, and N_2 (Eq. (17), Table 1). The oxygen diffusion exchange function $f(O_2)$ (Eq. (18), Table 1), which is dependent on the volumetric anaerobic fraction of the soil (Eq. (16), Table 1), and the oxygen diffusion reduction parameter both governing the exchange from anaerobic sites to aerobic sites. Oxygen diffusion rate (O_r), which is dependent on the tortuosity of the gas d_{O_2}, air-filled porosity f_a, oxygen diffusion rate specifically at 20 °C o_{dc} (=2.6 e^{-5} m^2 s^{-1} (Welty et al., 1984)), and diffusion coefficient in free air D, are calculated in Eq. (19) (Table 1).

2.7. *Model parameterisation and validation*

In order to parameterise CoupModel for nitrous gas emissions, three options (A–C) were selected. The time resolution for input variables in the simulations was daily mean values and the model was pre-running for 3 months to stabilise the initial conditions. Option A was performed with the same parameter setup as the PnET-N-DNDC model simulation using the nitrogen gas emissions in Eq. (18) (Table 1). Option B was carried out with a base parameter change from 0 to 0.00005 in the oxygen exchange function (o_b in Eq. (20), Table 1). The value was found by testing the hypotheses that denitrification produced gases are emitted in all moisture conditions in soils by changing in Eq. (18) to provide reasonable agreement during the winter period (Fig. 2). Differences between options A and B in the function of oxygen diffusion exchange due to the added base parameter are shown in Fig. 3.

The model is conceptually viewed as an aerobic site where nitrification process and transport of gases takes place, and an anaerobic site, where denitrification takes place (Fig. 1). The parameter o_b in Eq. (20) was added to provide an opportunity for the system to emit gases from the anaerobic site even when the soil was fully occupied by the anaerobic fraction. This is used to account for heterogeneity within the soil in a broader perspective, and is particularly important for CoupModel, which can be set to explicitly account for the gas transport within completely saturated soils. Experience through, demonstrates that soils with shallow ground water are never completely saturated. Normally, field saturation is well below the full porosity value. This means that high heterogeneity is a result of temporally saturated soils. Our new concept is an empirical way of accounting for transport within one layer, that is, from the anaerobic to the aerobic site. The vertical transport of gases will, in the model, be calculated as diffusion based on a steady state assumption between the produced net fluxes (from the anaerobic to the aerobic site). No dynamic storage of gases is accounted for within the soil. The exchange depends on the anaerobic volume fraction with o_b as the minimum exchange when the anaerobic volumetric fraction is 0 or 100%, conceptually leaving a column for transporting denitrified gases up through the soil. In option A the setup was $o_d = 0.01$ and $o_b = 0$, while in option B $o_d = 0.0005$ and $o_b = 0.00005$ (Fig. 3). Finally, the trace gas emissions to the atmosphere are calculated as the sum of gas formed during nitrification and the gas transported to the aerobic site after its formation during denitrification.

A third simulation, option C, was selected to test the dependence of NO and N_2O emission rates on the availability of nitrogen during freezing/thawing episodes. The added dry N deposition was 0.2 g m^{-2} day^{-1}, and 0.65:0.35 in NH_4^+:NO_3^- ratio. Secondly, the initial humus amount was reduced by 80%, compensating for the high amount of mineral N to maintain the total amount of N in the system.

3. Results and discussion

The simulated accumulated amount of NO and N_2O emitted during the period July 1995 to July 1996 generally resulted

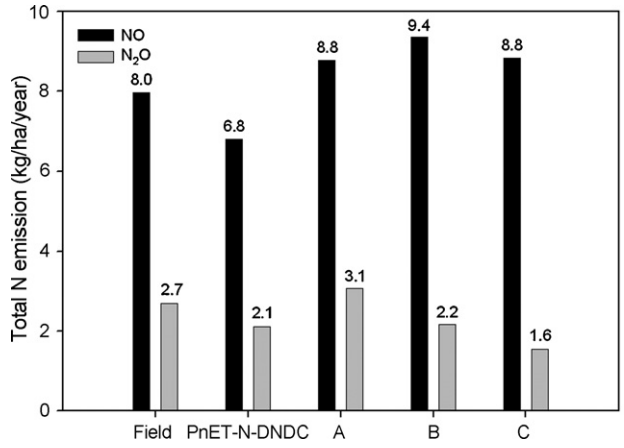

Fig. 4 – NO and N_2O total emissions for 1 year (July 1995 to July 1996) from field measurements and the four simulated options.

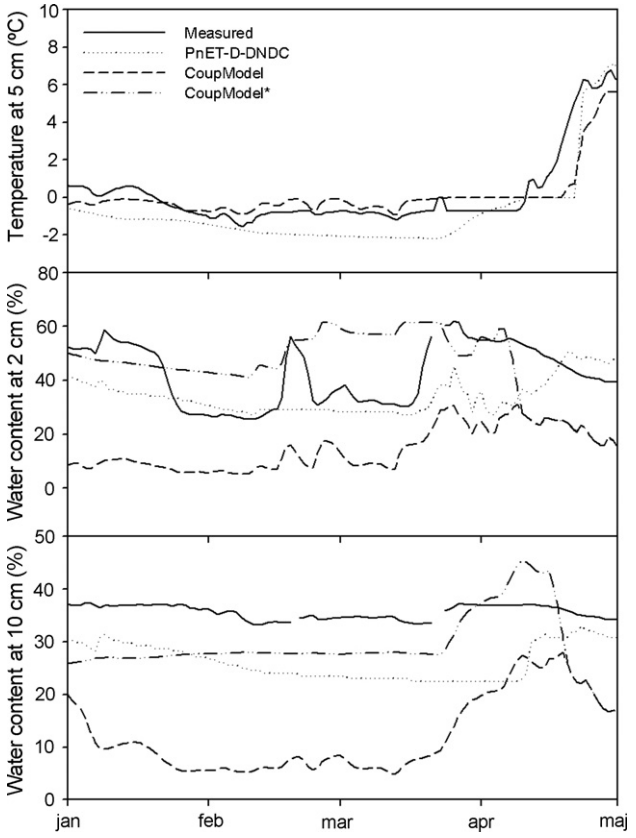

Fig. 5 – Temperature at 5 cm depth for measured data (solid line), PnET-N-DNDC (dotted line) and CoupModel option A and B (dashed line). Water content at 2 and 10 cm depth for measured data (solid line), PnET-N-DNDC (dotted line), CoupModel option A and B (dashed line) and total water content (ice plus liquid water) for CoupModel* option A and B (dash-dotted line). All graphs during the freezing/thawing period 1 January to 1 May.

in small differences between the different model setups and measured data (Fig. 4). However, the differences between the models did affect the time series of emission pattern and estimations of NO and N_2O. The total NO emission simulations with CoupModel (option A, B, and C) resulted in overestimations (10%, 18% and 10%, respectively), while for PnET-N-DNDC it resulted in an underestimation (−15%). For total N_2O emissions, the CoupModel simulations resulted in an overestimation for option A (15%), and underestimations for option B and C (−19% and −41%), compared with the measured data. This was also the case for PnET-N-DNDC (−22%). Obviously, it is a great challenge to model NO and N_2O fluxes on a yearly basis, as has also been shown in earlier studies. For example Henault et al. (2005), who modelled N_2O emissions from agriculture by the NOE model (an algorithm for assessing N_2O emissions from field scale), overestimated the flux by approximately 50% for three out of five sites, whereas Parton et al. (2001) slightly underestimated N_2O flux and overestimated NO flux for a grassland site on a sandy loam. However, the year chosen here from the Höglwald Forest databank for model testing was an especially difficult one. High fluxes of N_2O in February to March occurred during a prolonged period of frost, with several intermediate periods of surface thawing (Papen and Butterbach-Bahl, 1999) (Fig. 2). The field data for soil temperature at 5 cm depth in Fig. 5 can be easily linked to N_2O emissions in Fig. 2.

All simulations described temporal dynamics in emissions of NO and N_2O rates similar to the field measurements shown in Fig. 2, and had an r^2 between 0.39 (option A) and 0.54 (option C) for NO, and 0.26 (option B) and 0.57 (PnET-N-DNDC) for N_2O, except N_2O emission rate for option A with ($r^2 = 0.01$) (Table 4). Neither of the simulations had an offset in the potential to describe the measured data ($\beta_0 = 0.00$), but the linear slopes for all simulations indicate that the models experienced difficulties in describing high measured emission values during the freezing period. For NO, β_1 was between 0.33 (PnET-N-DNDC) and 0.61 (option C), while for N_2O β_1 was between 0.25 (option C) and 0.86 (option B).

The simulated NO and N_2O emission rates for options A and B and the already published PnET-N-DNDC simulation, as well as the field data (Stange et al., 2000), are graphically presented in Fig. 2. Almost no differences in emission rate of NO were found between options A and B (Fig. 2), but both simulation models showed a temporal delay in relation to the field measurements. Most of the modelled NO was produced during the nitrification process in both summer and winter (Fig. 6), which rules out denitrification as a major source of NO production. However, the results from option C, with added nitrogen deposition, differed from those of options A and B, and also correlated best with the measured data (Table 4). From these results, we were able to conclude that an increase in available inorganic nitrogen (NH_4^+ and NO_3^-), as in option C, was able to describe the measured NO data better. The reason could be that humus content, N deposition or NO production was not measured properly or rather that the parameterisation of NO production in the model is incorrect. Thus, the time delay in NO emissions for options A and B, starting in April, is most likely due to a limitation in available NH_4^+ for the nitrification process. A possible explanation is that during this period, the

Table 4 – Linear regression for field data vs. simulated data (options A, B, C and PnET-N-DNDC) for temperature, WFPS, N_2O and NO emission rates from the soil

	Emission rate		Temperature		WFPS	
	NO	N_2O	5 cm	10 cm	2 cm	10 cm
Simulation A						
r^2	0.39	0.01	0.96	0.96	0.13	0.17
β_0	0.00	0.00	−0.63	−0.74	0.13	−0.09
β_1	0.52	0.77	1	0.99	0.45	0.72
Simulation B						
r^2	0.39	0.26	0.96	0.96	0.13	0.16
β_0	0.00	0.00	−0.63	−0.74	0.13	−0.08
β_1	0.52	0.86	1	0.99	0.46	0.71
Simulation C						
r^2	0.54	0.26	0.96	0.96	0.08	0.00
β_0	0.00	0.00	−0.63	−0.74	0.26	0.45
β_1	0.61	0.25	1	0.99	0.27	−0.04
PnET-N-DNDC						
r^2	0.44	0.57	0.98	0.97	0.24	0.00
β_0	0.00	0.00	−1.31	−1.17	0.24	0.52
β_1	0.33	0.39	1.28	1.21	0.52	0.09

Observed vs. predicted ($y = \beta_0 + \beta_1 x$).

competition for NH_4^+ and NO_3^- between plants and microbes is greatest (Zhang et al., 2002a; Dinnes et al., 2002).

The simulation of N_2O emission rate using option A could not replicate the measured data, and resulted in two extremely high and narrow peaks during the winter period (Fig. 2). However, option B resulted in a substantial improvement in the results as it generated two peaks in the winter period, where the first peak was larger than the second, which was closer to the field measurements. The reason for the differences between options A and B is that most of N_2O was formed during denitrification, at least in the winter period when most of the N_2O was emitted (Fig. 6). This is directly related to the gas exchange between the anaerobic and aerobic zones, which for option B has an exchange rate despite the anaerobic volume being 0% or 100% in the soil, while option A lacks an exchange rate for those occasions.

Option C, with high amounts of available nitrogen in the soil, generated an increase in the N_2O emission rate in February, instead of March as for options A and B (not shown in Fig. 2). The simulation also generated both higher and wider peaks in N_2O emissions for option C. The sevenfold higher addition of nitrogen deposition in option C compared with options A and B reduced the mineralisation of organic nitrogen by approximately 90%, and contributed to an accumulation of nitrogen in spruce trees (Table 5). The high addition of nitrogen also contributed to an increased leaching of mineral nitrogen from the system. Option C indicated that nitrogen deposition in this ecosystem contributed to the important competition between microbes and plants. The nitrogen balance for the system (Table 5) describes the potential of CoupModel to turn over and accumulate nitrogen. Options A, B and C all had a similar nitrogen balance, which at the end of the year ended up as a surplus.

CoupModel has a well-developed soil heat transport process, and all three simulations resulted in accurately described soil temperatures in relation to the measured data at two depths (Table 4). Similarly, water transfer, including water content in the soil profile, is a base process in CoupModel (Jansson and Karlberg, 2004). Fig. 5 shows that the simulation of CoupModel option A/B, as well as the PnET-N-DNDC simulation, had continually lower water content than the measured water content during the winter period (January to May). However, the output of total water content (ice and water) for CoupModel indicated a higher content than the measured value. Despite this, options A, B and C generally produced a lower mean level for WFPS, with a good temporal variation for options A and B (Table 4). At 10 cm depth, options A, B and C underestimated WFPS by approximately 40%, while the PnET-N-DNDC model only underestimated WFPS by about

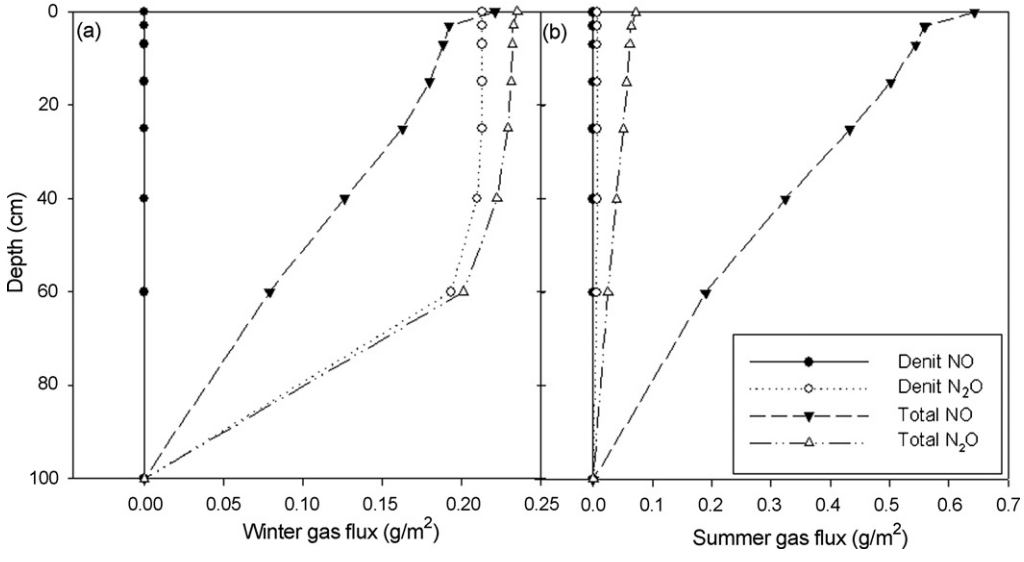

Fig. 6 – Seasonal gas flux of NO and N_2O emissions for option B (0–100 cm depth) from denitrification, and total emissions from both nitrification and denitrification, for (a) winter and (b) summer.

Table 5 – Accumulated nitrogen and nitrogen balance in the system during 1 year (1995–1996) for options A, B and C

Accumulated nitrogen	Amount (g N)		
	Simulation A	Simulation B	Simulation C
N deposition	+10.7	+10.7	+76.6
N difference in plants	−0.7	−0.7	+8.1
Difference in organic N in soil	−42.0	−41.9	−4.7
Difference in mineral N in soil	+36.4	+36.4	+46.0
N-emissions	−0.5	−0.5	−0.2
Dissolved organic N leaching	−1.9	−1.9	−2.4
Mineral N leaching	−5.1	−5.1	−17.9
Nitrogen balance in the system	+9.4	+9.3	+6.7

5% in the winter and spring period (Stange et al., 2000). However, options A and B described the temporal variation over time in accordance to the field data, and had values closer to the measured, compared with option C and PnET-N-DNDC (except for the simulation with PnET-N-DNDC at 2 cm depth). The difference in WFPS between options A/B, and C is probably due to less humus in the soil, which contributed to decreased porosity in option C. The reason way humus was added after adding only dry N deposition, was because the run resulted in a fivefold higher peak and annual accumulated N emission of NO was twofold and N_2O was sevenfold higher than measured. This large amount of available nitrogen was compensated for by reducing the initial amount of humus in the humus pool by 80% to maintain the total amount of nitrogen in the system.

Estimating WFPS is not only a complex issue for CoupModel and PnET-N-DNDC, but also for other models, e.g. the DAYCENT model (Parton et al., 2001), which underestimated WFPS values in the winter due to snowmelt runoff. This was corrected with a 'snowmelt algorithm' based on the daily maximum soil temperature, instead of daily mean soil temperature. However, the CoupModel simulations did not generate as accurate results as the other models, despite the well-simulated water content and temperature for the soil at other sites (Jansson et al., 2005). This indicates that the model's driving soil moisture parameters were inaccurate. CoupModel does not necessarily need more input data but it provides a more detailed description of the soil system, including ice and liquid-filled pore space. If this condition is only implicitly assumed we have a substantial structural uncertainty in the model. Difference in WFPS for the options could also indicate that N deposition, soil humus content, water content, and/or NO production, were not measured properly. But N deposition and humus content were properly measured at the Höglwald site (Kreutzer, 1995). The NO flux rate measurements has high temporal resolution, and the mean NO emission rate per day was calculated from 120 measuring points (annual mean rate was 8.7 ± 0.3 kg NO N kg ha^{-1} year^{-1} 1995 and 9.1 ± 0.4 kg NO N kg ha^{-1} year^{-1} at 1996) (Gasche and Papen, 1999), whereas the TDR moisture measurements are very variable in terms of magnitude with differences of 13% between probes (Rothe, 1997). This discrepancy, and the fact that there have been some instrument failures during the time of measurements (Rothe, 1997), leads to an inaccurate data set difficult to use as validation variables.

The thawing in April coincided with high water content and larger amounts of available nitrogen for the denitrification microbes. This may explain for the peaks in N_2O emission rate. Teepe et al. (2001) obtained similar results from a freezing/thawing laboratory study concerned with CO_2 and N_2O emissions. They found that the N_2O emission rate increased when the temperature decreased from +10 °C to −6 °C (for the topsoil), continuously increased during the period when soil temperature was below 0 °C, and ended with a high peak at the thawing period. Öquist et al. (2004) also found that large amounts of N_2O were emitted when the temperature was below 0 °C, presumable not only as an effect of thawing events. This correlates well with high soil moisture, which is in accordance with field data (Fig. 6b).

The advantage of option B in predicting NO and N_2O emission rates was that gas production reactions were governed by smaller scale changes in the soil physics. Small changes in soil moisture or temperature contributed to large changes in N emissions in the model.

The simulation of emitted N_2O and NO from denitrification and nitrification for option B showed large differences in summer (May to October), and winter (November to April) (Fig. 6). For N_2O emission it was easy to distinguish differences between winter and summer. In the winter period, N_2O was mainly emitted from the denitrification process, whereas in the summer period almost all N_2O stemmed from the nitrification process. Dividing the total NO and N_2O emissions into summer and winter periods also distinguished differences in results relating to depths between options A and B (Fig. 7). The largest deviation was discovered in the uppermost layer for both NO and N_2O emissions. Deeper in the soil profile there were almost no differences in N_2O exchange for the two models, for either of the seasons. It is clear that almost all emitted NO originated from the nitrification process during both the winter and summer period. For option B, NO emission increased more with depth than for option A in the winter period, but was the same for both options (from 3 to 100 cm depth) during the summer.

As regards the exact location of exchange of gaseous NO and N_2O between anaerobic and aerobic sites in the soil profile Gilliam et al. (1978) showed in a laboratory study that the most intense denitrification occurred at 30–75 cm depth in the soil profile. The CoupModel simulations produced similar results, with denitrification rates increasing with depth (Fig. 8). Unfortunately no model validation data were available for 30–75 cm depth to confirm this result. Compared with option A, option B generated smaller diffusion values for all anaerobic volume fractions, except for those near 0 and 1 (Fig. 2). The differ-

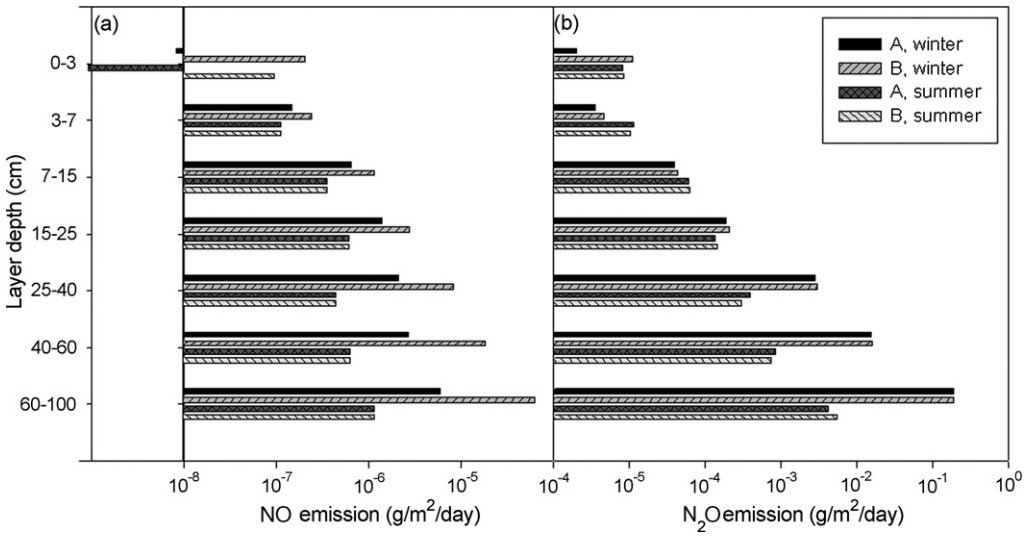

Fig. 7 – Mean emissions of (a) NO and (b) N_2O during winter and summer for options A and B in each layer down to 1 m depth.

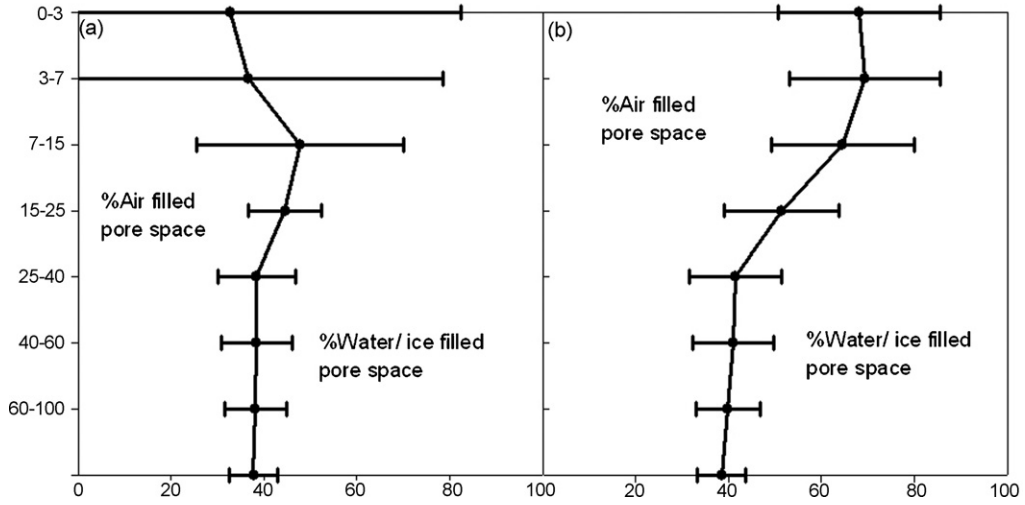

Fig. 8 – Mean values with two standard deviations of air- and water/ice-filled pore space in the profile for (a) winter and (b) summer.

ent parameter setup for the gas exchange function in options A and B results indirectly resulted in emissions of NO and N_2O in the uppermost layer (0–3 cm). For NO, this was true for both summer and winter periods, but for N_2O it was only true for the winter period (Fig. 7). This is most likely because the upper soil layer has a tendency to be either almost completely saturated due to precipitation events, or have all pores filled with air. Another reason is that 10-fold more N_2O is emitted from organic soil (uppermost layers) than from mineral soils (Menyailo and Huwe, 1999). The large abundance of water- or ice-filled pore space with depth is presented in Fig. 8. Deeper in the soil profile the only differences between options A, and B were in NO emission rate in the winter season (Fig. 7). This is because of generally wetter microclimate conditions below 15 cm, resulting in less than 70% air-filled pores (Fig. 8). According to Bateman and Baggs (2005), the flux of N_2O from denitrification increases, from a low N_2O production level at WFPS 0.6 to a maximum flow at WFPS 0.7, when all N_2O is produced during denitrification. Modifications made in option B enabled the model to take into account gas diffusion in the uppermost soil layer, with an abundance of organic material.

4. Conclusions

Even though the PnET-N-DNDC and CoupModel are different in many respects, the basic part of the nitrification/denitrification submodel was possible to transfer from the PnET-N-DNDC model to the CoupModel. The implementation of the PnET-N-DNDC submodel enhanced the capacity of CoupModel in predicting N_2O emissions. One major adjustment of the anaerobic balloon description was necessary to obtain reasonable good results when using the CoupModel. A

new base parameter allowing an exchange of N gases from the conceptual anaerobic to aerobic site, which aim to describe the heterogeneity in the soil when the soil is close to saturation. The amounts of annually accumulated NO emission were close to equal for the different CoupModel simulations. Most of the NO was formed during nitrification while the N_2O was mostly formed during denitrification. Thus, the concept used in PnET-N-DNDC seems to be a robust construction for flux estimates. However, further work is needed to parameterise and investigate the uncertainty of simulated for NO and N_2O emissions by using the current version of the CoupModel.

Acknowledgements

This research was conducted with the Graduate School of Climate and Mobility at Gothenburg University, and financially supported by the Swedish Research Council for Environment, Agricultural Sciences and Spatial Planning (grants 22.0/2004-0449 and 21.0/2004-0518), and the Swedish Research Council (grant no. 621-2003-2730). Leif Klemedtsson's contribution was provided within the *Land use strategies for reducing net greenhouse gas emissions* project, supported by the Foundation for Strategic Environmental Research (MISTRA). This is publication No. 19 from Tellus – the Centre of Earth Systems Science at the University of Gothenburg. The work was supported by the EU project Nitrogen Europe. The authors express their gratitude to Stephan Andersson for valuable comments on the manuscript. All are gratefully acknowledged.

REFERENCES

Aber, J.D., Federer, C.A., 1992. A generalized, lumped-parameter model of photosynthesis, evapotranspiration and net primary production in temperate and boreal forest ecosystems. Oecologia 92, 463–474.

Bateman, E.J., Baggs, E.M., 2005. Contributions of nitrification and denitrification to N_2O emissions from soils at different water-filled pore space. Biology and Fertility of Soils 41, 379–388.

Baumgartner, M., Conrad, R., 1992. Effects of soil variables and season on the production and consumption of nitric-oxide in oxic soils. Biology and Fertility of Soils 14, 166–174.

Breuer, K.S., Koseff, J.R., Powell, K., Robertson, C., January 2000. Multimedia Fluid Mechanics, CD-ROM edition. Cambridge University Press.

Butterbach-Bahl, K., Gasche, R., Bruer, L., Papen, H., 1997. Fluxes of NO and N_2O from temperate forest soils: impact of forest type, N deposition and of liming on the NO and N_2O emissions. Nutrient Cycling in Agroecosystems 48, 79–90.

Butterbach-Bahl, K., Gasche, R., Huber, Ch., Kreutzer, K., Papen, H., 1998. Impact of N-input by wet deposition an N-trace gas fluxes and CH_4-oxidation in spruce forest ecosystems of the temperate zone in Europe. Atmospheric Environment 32, 559–564.

Butterbach-Bahl, K., Kesik, M., Miehle, P., Papen, H., Li, C., 2004. Quantifying the regional source strength of N-trace gases across agricultural and forest ecosystems with process based models. Plant and Soil 260, 311–329.

Conen, F., Dobbie, K.E., Smith, K.A., 2000a. Predicting N_2O emissions from agricultural land through related soil parameters. Global Change Biology 6, 417–426.

Conen, F., Dobbie, K.E., Smith, K.A., 2000b. Predicting N_2O emissions from agricultural land through related soil parameters. Global Change Biology 4, 417–426.

Dinnes, D.L., Karlen, D.L., Jaynes, D.B., Kaspar, T.C., Hatfield, J.L., Colvin, T.S., Cambardella, C.A., 2002. Nitrogen management strategies to reduce nitrate leaching in tile-drained Midwestern soils. Agronomy Journal 94, 153–171.

Eckersten, H., Jansson, P.E., Johnsson, H., 1998. SOILN Model, Version 9.2, User's Manual. Swedish Agricultural University, Uppsala.

Firestone, M.K., Davidson, E.A., 1989. Microbiological basis of NO and N_2O production and consumption in soil. In: Andreae, M.O., Schimel, D.S. (Eds.), Exchange of Trace Gases between Terrestrial Ecosystems and the Atmosphere. John Wiley and Sons Ltd., pp. 7–21.

Gasche, R., Papen, H., 1999. A 3-years continuous record of trace gas fluxes from untreated and limed soil of a N-saturated spruce and beech forest ecosystem in Germany. 1. NO and NO_2 fluxes. Journal of Geophysical Research-Atmospheres 104, 18505–18520.

Gilliam, J.W., Dasberg, S., Lund, L.J., Focht, D.D., 1978. Denitrification in four California soils: effect of soil profile characteristics. Soil Science Society of America Journal 42, 61–66.

Henault, C., Germon, J.C., 2000. NEMIS, a predictive model of denitrification on the field scale. European Journal of Soil Science 51, 257–270.

Henault, C., Bizouard, F., Laville, P., Gabrielle, B., Nicoullaud, B., Germon, J.C., Cellier, P., 2005. Predicting in situ soil N_2O emission using NOE algorithm and soil database. Global Change Biology 11, 115–127.

Ingwersen, J., Butterbach-Bahl, K., Gasche, R., Richter, O., Papen, H., 1999. Barometric process separation: new method for quantifying nitrification, denitrification, and nitrous oxide sources in soils. Soil Science Society of America Journal 63, 117–128.

IPCC, 2001a. Climate Change: Mitigation. Cambridge University Press, Cambridge.

IPCC, 2001b. Climate Change: The Scientific Basis Contribution. Cambridge University Press, Cambridge.

Jansson, P.E., Halldin, S., 1979. Model for Annual Water and Energy Flow in a Layered Soil. Society for Ecological Modelling, Copenhagen, p. 145.

Jansson, P.E., Karlberg, L., 2004. Coupled heat and mass transfer model for soil-plant-atmosphere systems. Royal Institute of Technology, Dept. of Land and Water Resources Engineering Stockholm, Sweden, Publication 427.

Jansson, P.E., Moon, D.S., 2001. A coupled model of water, heat and mass transfer using object orientation to improve flexibility and functionality. Environmental Modelling and Software 16, 37–46.

Jansson, C., Espeby, B., Jansson, P.E., 2005. Preferential water flow in a glacial till soil. Journal of Nordic Hydrology 36, 1–11.

Johnsson, H., Bergström, L., Jansson, P.-E., 1987. Simulated nitrogen dynamics and losses in a layered agricultural soil. Agriculture Ecosystems and Environment 18, 333–356.

Kreutzer, K., 1995. Effects of forest liming on soil processes. Plant and Soil 169, 447–470.

Langeveld, C.A., Leffelaar, P.A., 2002. Modelling belowground processes to explain field-scale emissions of nitrous oxide. Ecological Modelling 149, 97–112.

Li, C.S., Frolking, S., Frolking, T.A., 1992. A model of nitrous-oxide evolution from soil driven by rainfall events. 1. Model structure and sensitivity. Journal of Geophysical

Research-Atmospheres 97, 9759–9776.
Li, C., Aber, J.D., Stange, F., Butterbach-Bahl, K., Papen, H., 2000. A process-oriented model of N_2O and NO emissions from forest soils. 1. Model development. Journal of Geophysical Research 105, 4369–4384.
Maag, M., Vinther, F.P., 1996. Nitrous oxide emission by nitrification and denitrification in different soil types and at different soil moisture contents and temperatures. Applied Soil Ecology 4, 5–14.
Menyailo, O.V., Huwe, B., 1999. Denitrification and C, N mineralization as a function of temperature and moisture potential in organic and mineral horizons of an acid spruce forest soil. Journal of Plant Nutrition and Soil Science-Zeitschrift Fur Pflanzenernahrung Und Bodenkunde 162, 527–531.
Öquist, M.G., Nilsson, M., Sorensson, F., Kasimir-Klemedtsson, A., Persson, T., Weslien, P., Klemedtsson, L., 2004. Nitrous oxide production in a forest soil at low temperatures—processes and environmental controls. Fems Microbiology Ecology 49, 371–378.
Papen, H., Butterbach-Bahl, K., 1999. A 3-years continuous record of trace gas fluxes from untreated and limed soil of a N-saturated spruce and beech forest ecosystem in Germany. 1. N_2O emissions. Journal of Geophysical Research-Atmospheres 104, 18487–18503.
Parton, W.J., Holland, E.A., Del Grosso, S.J., Hartman, M.D., Martin, R.E., Mosier, A.R., Ojima, D.S., Schimel, D.S., 2001. Generalized model for NO_x and N_2O emissions from soils. Journal of Geophysical Research-Atmospheres 106, 17403–17419.
Potter, C., Davidson, E., Nepstad, D., de Carvalho, C.R., 2000. Ecosystem modeling and dynamic effects of deforestation on trace gas fluxes in Amazon tropical forests. Forest Ecology and Management 152, 97–117.
Robertson, G.P., 1989. Nitrification and denitrification in humid tropical ecosystems: potential controls on nitrogen retention. In: Procter, J. (Ed.), Mineral Nutrients in Tropical Forest and Savanna Ecosystems. Blackwell Scientific, Oxford, pp. 55–70.
Rothe, A., 1997. Einfluss des Baumartenanteils auf Durchwurzelung, Wasserhaushalt, Stoffhaushalt und Zuwachsleistung eines Fichten-Buchen-Mischbestandes am Standort Höglwald. Forstliche Forschungsberichte München 163, 1–174.
Stange, F., 2001. Entwicklung und Anwendung eines prozessorientierten Modells zur Beschreibung der N_2O- und NO-Emissionen aus Böden temperater Wälder. Fraunhofer Institut Atmosphärische Umweltforschung, Schriftenreihe Band 69–2001, Garmisch-Partenkirchen.
Stange, F., Butterbuch-Bahl, K., Papen, H., Zechmeister-Boltenstern, S., Li, C., Aber, J.D., 2000. A process-oriented model of N_2O and NO emissions from forest soils. 2. Sensitivity analysis and validation. Journal of Geophysical Research 105, 4385–4398.
Teepe, R., Brumme, R., Beese, F., 2001. Nitrous oxide emissions from soil during freezing and thawing periods. Soil Biology and Biochemistry 33, 1269–1275.
Tiktak, A., van Grinsven, H.J.M., 1995. Review of sixteen forest–soil-atmosphere models. Ecological Modelling 83, 35–53.
Van Verseveld, H.W., Meijer, E.M., Stouthamer, A.H., 1977. Energy conservation during nitrate respiration in *Paracoccus denitrificans*. Archives of Microbiology 112, 17–23.
Welty, J.R., Wicks, C.E., Wilson, R.E., 1984. Fundamentals of Momentum, Heat, and Mass Transfer, 3rd ed. John Wiley & Sons, NY, p. 803.
Zhang, Y., Li, C., Zhou, X., Moore, B., 2002a. A simulation model linking crop growth and soil biogeochemistry for sustainable agriculture. Ecological Modelling 151, 75–108.
Zhang, Y., Li, C.S., Trettin, C.C., Li, H., Sun, G., 2002b. An integrated model of soil, hydrology, and vegetation for carbon dynamics in wetland ecosystems. Global Biogeochemical Cycles 16, 1–18.